CHAPTER 2

Electrochemical Detection of Lesions in DNA

Adapted from Boal, A. K., and Barton, J. K. (2005) *Bioconjugate Chemistry 16*, 312.

INTRODUCTION

DNA is remarkably susceptible to chemical modification (*1-3*). Hydrolytic damage is the most common form of DNA base modification and often leads to deamination of cytosine and depurination. Oxidative damage results in a variety of base modifications, but 8-oxo-G is thought to be the most prevalent of these lesions. Non-enzymatic alkylation by endogenous and exogenous alkylating agents is also an important type of base damage (*2*). Modification of DNA bases can disrupt DNA replication and transcription by altering the base pairing properties of the DNA base and stalling the protein machinery associated with these processes. Base damage may also be an important indicator in the diagnosis and treatment of cancer, as high levels of damaged bases are often the result of exposure to carcinogens (*4*).

The base pair π-stack, formed when duplex DNA assumes a helical conformation, is capable of mediating charge transport (CT) (*5-9*). This chemistry is exquisitely sensitive to changes in base pair structure and dynamics; intervening mismatches in base pairing lead to a loss in the ability to transfer charge from an electron donor to an electron acceptor (*10*), as do bulges (*11*) or structural perturbations in base pair stacking induced by proteins (*12, 13*). While an *in vivo* role for DNA-mediated CT has yet to be established, it is interesting to consider that DNA-mediated CT may be involved in DNA damage and repair (*14*). Long range DNA-mediated CT provides a potential route for funneling oxidative damage to specific regions of the genome and insulating alternate regions (*14, 15*). We have proposed that DNA repair proteins may take advantage of the sensitivity of DNA-mediated CT to DNA structural modifications in order to scan the genome for damage as an efficient long range detection scheme (*14, 16*).

The remarkable sensitivity of DNA-mediated CT to perturbations in base pair stacking and dynamics suggested that this chemistry could be applied in the design of sensors that detect base pair mismatches and damage products. Our laboratory has developed one such sensor for the detection of single base mutations in duplex DNA (*17, 18*). In this device, a monolayer of thiol-terminated DNA oligonucleotide duplexes is assembled on a gold surface; a redox-active intercalator bound near the top of the film acts as the probe of DNA CT chemistry. The DNA-mediated reduction of the intercalator is easily monitored electrochemically if the DNA is fully Watson-Crick base paired. However, the presence of a single base pair mismatch or other structural perturbation within the base pair stack attenuates intercalator reduction. This sensor is unique in that it does not exploit differences in hybridization thermodynamics to detect mutations, but instead differences in electronic coupling within the π-stack. Greater sensitivity to perturbations in the π-stack is attained by coupling the DNA-mediated reduction of the intercalative probe into an electrocatalytic cycle with an oxidant in solution capable of re-oxidizing the intercalator. Figure 2.1 illustrates this cycle utilizing the intercalator methylene blue as the electrocatalyst for ferricyanide reduction. The integrity of the DNA π-stack is repeatedly probed via electron transfer in this catalytic cycle, and thus any perturbations in base pair stacking are amplified. Using this methodology, all single base mismatches in DNA, irrespective of sequence context or thermal stability, can be readily detected (*18*). Indeed recently, a full range of DNA-based biosensors have been developed (*19,20*).

Here we examine the scope of this methodology. We are interested in determining the primary factors governing the detection of DNA lesions by DNA charge transfer chemistry and the range of lesions that may be detected. How effective, for

Figure 2.1. Scheme for electrocatalysis at a DNA-modified electrode. MB^+ denotes methylene blue as the redox-active intercalative probe. MB^+ is reduced to leucomethylene blue (LB^+) in a DNA-mediated electron transfer process. Ferricyanide ($Fe(CN)_6^{3+}$) is oxidized by LB^+ to regenerate the redox-active intercalative probe.

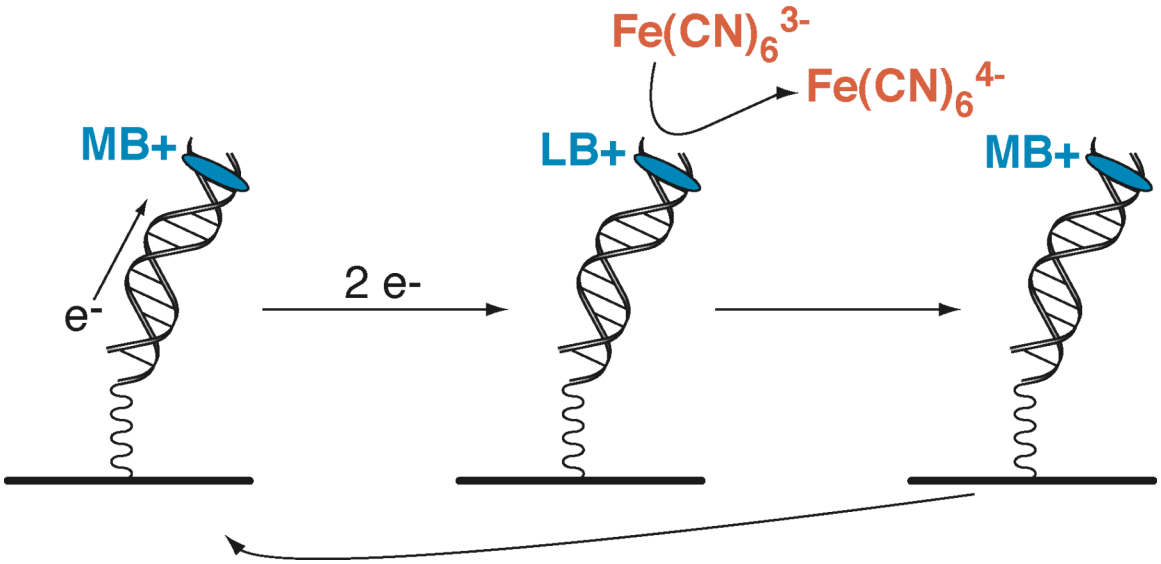

example, is this chemistry in detecting DNA methylation? Are base analogues utilized as probes of nucleic acid processes or as therapeutics readily detected? We have already observed that the conformational distortions in synthetic oligonucleotides containing constrained sugar-phosphate backbones can be detected electrochemically (*21*), and this may be an important consideration in their application in antisense therapeutics. Perhaps most importantly, our understanding of the sensitivity and scope of DNA CT chemistry in the detection of lesions provides a foundation for the consideration of possible roles for DNA CT in mechanisms of DNA repair.

MATERIALS AND METHODS

Materials

All reagents for DNA synthesis were purchased from Glen Research (including all unnatural DNA base phosphoramidites). Methylene blue, ferricyanide, and reagents used in the synthesis of thiol-modified DNA were purchased from Aldrich in the highest available purity and used as received. All buffers were prepared with Milli-Q water and filtered with a sterile, 0.2 μm filter.

Preparation of DNA-modified Electrodes

Oligonucleotides were prepared using standard phosphoramidite synthesis on an ABI 392 model DNA synthesizer. Oligonucleotide composition was verified by mass spectrometry. Thiol-modified duplexes were prepared using a solid-phase coupling procedure (*17*). The modified DNA was HPLC-purified on a semi-preparative C18 column after either the amino modification or attachment of the disulfide moiety and again after the thiol deprotection. Thiol-modified DNA and the appropriate

complementary strand were prepared in a 100 μM solution and annealed on a thermocycler. The resulting duplexes were self-assembled overnight (12-24 hours) on polished (0.3 μm, 0.05 μm alumina) and etched (CV from +1575 mV to -250 mV, 20 cycles in 1M H_2SO_4) bulk gold electrodes. $MgCl_2$ (100 mM) was added to the DNA solution prior to incubation to ensure a well-packed film. All DNA films were confirmed to be densely packed using a standard ferricyanide assay (*22*). At least three trials were performed for each base modification.

Electrochemical Analysis of DNA Films

Cyclic voltammetry and chronocoulometry experiments were carried out on a BAS CV50W model electrochemical analyzer. Experiments were executed in 50 mM NaCl, 5mM sodium phosphate, pH 7, at ambient temperatures under an inert atmosphere. A 3-compartment electrochemical cell was used with a Pt wire auxiliary electrode, 0.02 cm^2 gold working electrode, and saturated calomel reference electrode separated from the working electrode by a modified Luggin capillary.

Thermal Denaturation Studies

DNA duplexes (1.6 μM) were tested in 50 mM NaCl, 5 mM sodium phosphate, 100 mM $MgCl_2$, pH 7.0 in a quartz cell (with the exception of the lesions in group 4 which were analyzed in the absence of $MgCl_2$ and without the thiol tether). Absorbance at 260 nm was measured on a Beckman DU7400 spectrophotometer as the temperature decreased from 90 °C to 20 °C in a 0.5 °C/minute linear gradient. Melting curves were fit to a sigmoidal function using ORIGIN software. The T_m is defined as the midpoint of these sigmoidal curves.

RESULTS AND DISCUSSION

Methodology

Base lesions are incorporated into 15mer thiol terminated duplexes using standard phosphoramidite chemistry and the DNAs containing the base lesions are self-assembled into monolayers on gold electrodes. These DNA-modified electrodes are then investigated electrochemically using noncovalent methylene blue (MB) as a redox-active probe either directly or, in conjunction with ferricyanide, electrocatalytically. When MB is used as a direct probe, the DNA-modified electrodes are immersed in a buffered solution containing 2 μM MB. Note that it is the reduction of MB that is monitored using cyclic voltammetry from 0 to –650 mV; some of the lesions examined are easily oxidized but the conditions monitored here do not promote redox chemistry on the bases themselves. MB is also used as a catalytic reductive probe, when the DNA modified electrode is placed in a solution containing 2 mM ferricyanide and 0.5 μM MB. The redox activity of MB is then monitored primarily using chronocoulometry. In the experiments described here, charge is monitored for a period of 5s while the potential steps from 0 to –350 mV.

The lesions investigated here encompass a wide variety of modifications to DNA bases. Some of these lesions occur physiologically as a result of enzymatic modification to DNA or as a result of oxidative and/or hydrolytic damage. Other lesions represent synthetic modifications to DNA bases, damage to bases that is the result of exposure to alkylating agents, bases used as therapeutics, and fluorescent bases commonly used as synthetic probes of DNA.

Group 1 Lesions

The group 1 lesions are all associated with DNA damage processes. O4-methyl-thymine (OMT) and O6-methyl-guanine (OMG) are methylation damage products occurring at sites involved in hydrogen bonding, and 5-hydroxy-cytosine (OHC) and 8-oxo-guanine (OG) are common oxidative damage products (*23*). The structures of these lesions are shown in Figure 2.2. DNA films containing OMG base paired with cytosine can be distinguished electrochemically, either with or without electrocatalysis, from those containing well-matched unmodified base pairs (Figure 2.2). OMT base paired with adenine can also be detected with and without electrocatalysis, but detection is greatly enhanced using electrocatalysis. As illustrated in Table 2.1, incorporation of these lesions into DNA duplexes also leads to dramatically reduced T_m values. It is noteworthy, however, that duplexes containing OMG have a lower T_m than those containing OMT, yet show less attenuation in MB reduction.

The oxidative damage products OG and OHC can also be detected electrochemically both with and without electrocatalysis (Figure 2.2). OG is examined here base paired with both A and C (OG:A and OG:C, respectively). In both base pairing contexts, OG is detectable when MB is used as a direct probe. In the electrocatalysis experiments, OG is detectable when paired with C or A, but detection of OG:A is especially pronounced. OHC is also easily detectable with electrocatalysis. It is noteworthy that a higher background current is consistently observed in DNA films containing OHC; possibly this reflects a difference in film morphology. Note that all data, irrespective of film capacitance, were first background corrected.

Figure 2.2. Electrochemical detection of group 1 lesions. A. Cyclic voltammetry without electrocatalysis. B. Bar graph representing peak current attained in cyclic voltammetry experiments without electrocatalysis. C. Chronocoulometry with electrocatalysis. D. Structures of group 1 lesions. Deviations from standard base pairs are shown in red.

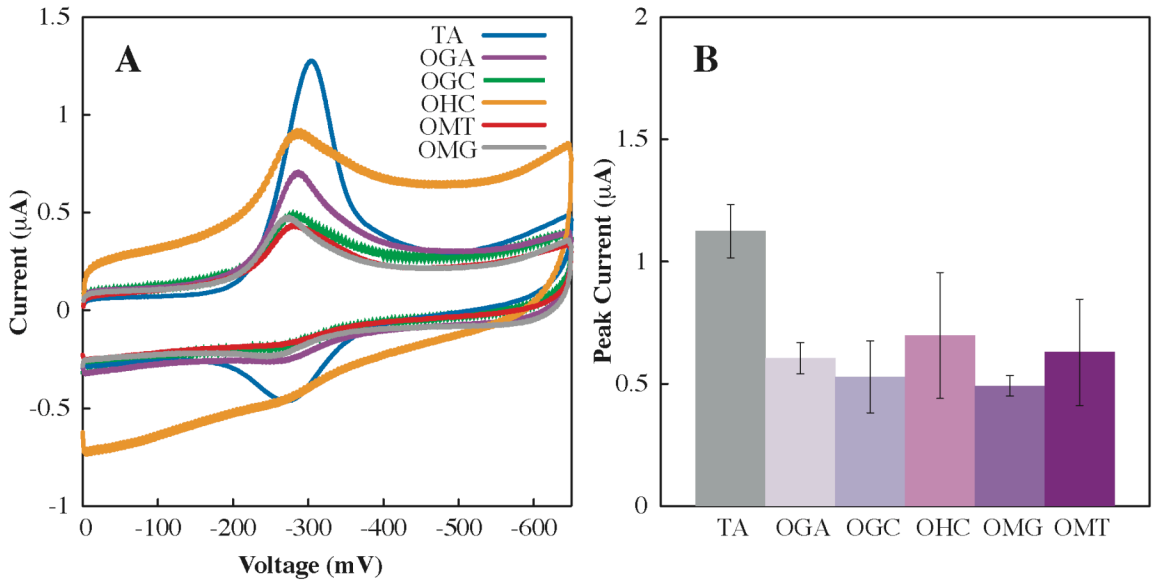

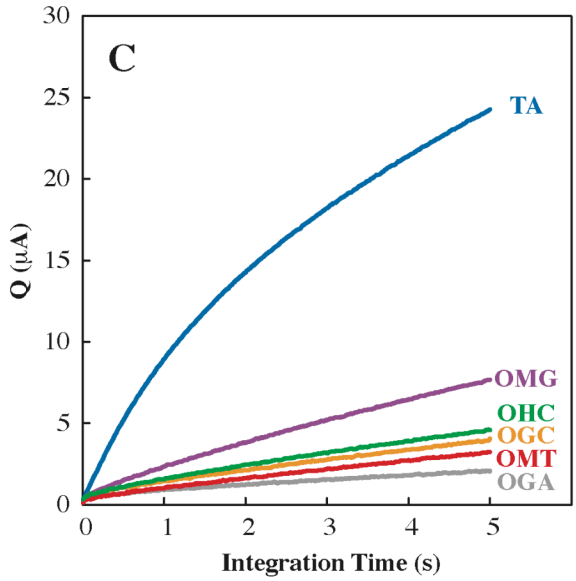

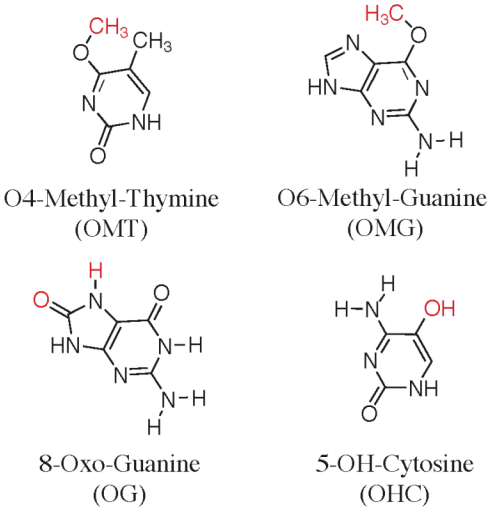

Table 2.1. Electrochemical detection of group 1 lesions.

Lesion	Sequence[a]	T_m (°C)	Q (μA) w/out electrocatalysis[b]	Q (μA) with electrocatalysis[c]
no lesion (TA)	SH - 5' - AGT ACA GTC ATC GCG 3' - TCA TGT CAG TAG CGC	60.0	1.27 ± 0.12	23.9 ± 1.7
O4-Methyl-Thymine (OMT)	SH - 5' - AGT ACA GTC ATC GCG 3' - TCA TG**T** CAG TAG CGC	49.4	0.63 ± 0.22	3.1 ± 1.0
O6-Methyl-Guanine (OMG)	SH - 5' - AGT ACA GTC ATC GCG 3' - TCA TGU CA**G** TAG CGC	47.8	0.492 ± 0.041	8.1 ± 2.4
5-Hydroxy-Cytosine (OHC)	SH - 5' - AGT ACA GTC ATC GCG 3' - TCA TGT **C**AG TAG CGC	54.9	0.70 ± 0.25	5.1 ± 1.1
8-Oxo-Guanine:C (OGC)	SH - 5' - AGT ACA GTC ATC GCG 3' - TCA TGT CA**G** TAG CGC	53.6	0.53 ± 0.15	4.1 ± 0.6
8-Oxo-Guanine:A (OGA)	SH - 5' - AGT ACA GTC ATC GCG 3' - TCA TG**G** CAG TAG CGC	52.3	0.604 ± 0.064	2.9 ± 0.5

[a] SH - 5' represents $SH(CH_2)_2CONH(CH_2)_6NHCO$ at 5'-OH
[b] Electrochemical detection using 2 μM methylene blue (MB) as redox probe. Q = current at CV peak.
[c] Electrochemical detection with electrocatalysis: 0.5 μM MB, 2 mM $Fe(CN)_6^{3-}$. Q = integrated current at 5s.

As evident in Table 2.1, these lesions are somewhat thermodynamically destabilizing; duplexes containing these modifications have lower melting temperatures than unmodified duplexes (TA). Nonetheless, incorporation of these lesions in DNA films leads to a dramatic attenuation in CT efficiency.

Group 2 Lesions

Group 2 includes the synthetic base analogues, P and K, that function as degenerate bases; they can pair with either purines (P) or pyrimidines (K) (*24*). Nebularine (Neb) is a natural product that also has greater base pairing degeneracy than the natural purines (*25*). As illustrated in Figure 2.3, each of these lesions causes a profound decrease in DNA-mediated CT monitored with electrocatalysis. Significantly, P and K base paired to each other results in a higher charge accumulation when compared to P or K base paired to a natural base. As evident in Table 2.2, it is also interesting that the duplex with the highest charge accumulation (Q) with electrocatalysis has the lowest T_m. This result provides another indication that CT attenuation does not correlate with duplex melting temperature.

Group 3 Lesions

This group includes the therapeutic base 5-fluoro-uracil (FIU) (*26*), fluorescent bases 2-amino-purine (2Ap) (*27*) and etheno-adenine (EA) (*28*), and synthetic base analogues 7-deaza-guanine (ZG) (*29*) and 7-deaza-adenine (ZA) (*30*). Group 3 represents structural modifications to DNA bases that are either completely synthetic (ZA, ZG, FIU, 2Ap) or the result of exposure to exogenous mutagens (EA).

Figure 2.4 illustrates, in DNA films containing these lesions, the reduction of MB without electrocatalysis as measured by cyclic voltammetry. None of these lesions are

Figure 2.3. Electrochemical detection of group 2 lesions. A. Cyclic voltammetry without electrocatalysis. B. Bar graph representing peak current attained in cyclic voltammetry experiments without electrocatalysis. C. Chronocoulometry with electrocatalysis. D. Structures of group 2 lesions. Deviations from standard base pairs are shown in red.

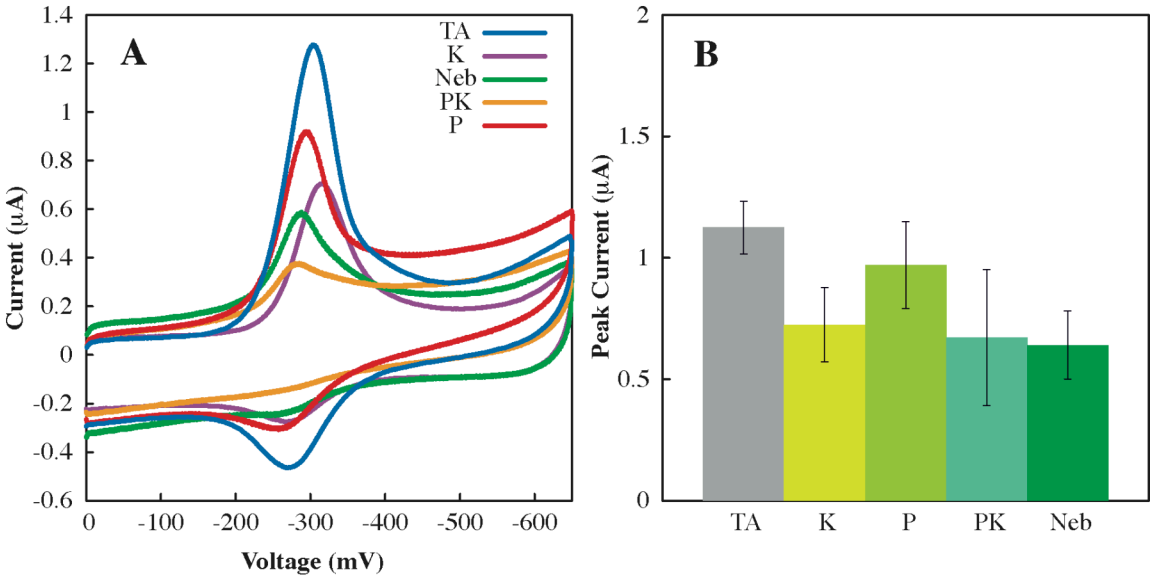

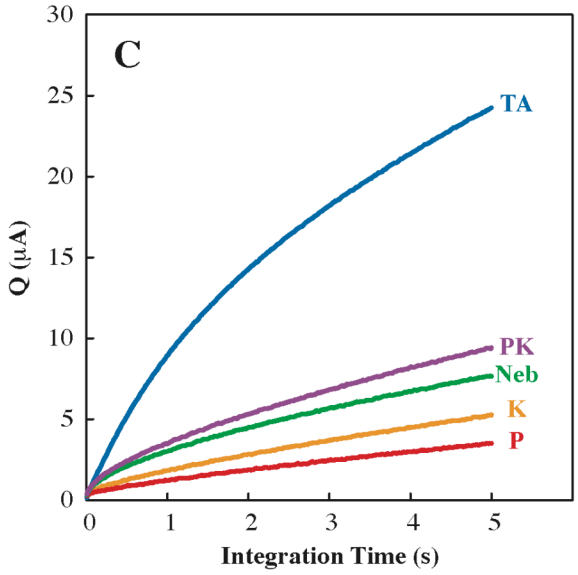

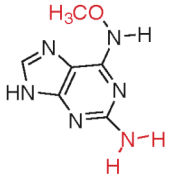

dK (K)

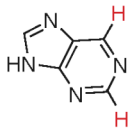

Nebularine (Neb)

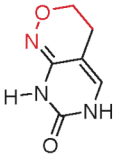

dP (P)

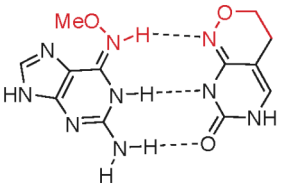

K:P (PK)

Table 2.2. Electrochemical detection of group 2 lesions.

Lesion	Sequence[a]	T_m (°C)	Q (μA) w/out electrocatalysis[b]	Q (μA) with electrocatalysis[c]
no lesion (TA)	SH – 5' – AGT ACA GTC ATC GCG 3' – TCA TGT CAG TAG CGC	60.0	1.27 ± 0.12	23.9 ± 1.7
dP (P)	SH – 5' – AGT ACA GTC ATC GCG 3' – TCA TG**P** CAG UAG CGC	56.8	0.97 ± 0.18	5.9 ± 2.2
dK (K)	SH – 5' – AGT ACA GTC ATC GCG 3' – TCA TGT C**K**G TAG CGC	53.4	0.73 ± 0.15	6.6 ± 2.5
P:K (PK)	SH – 5' – AGT ACA G**P**C ATC GCG 3' – TCA TGT C**K**G TAG CGC	50.2	0.67 ± 0.28	10.1 ± 2.1
Nebularine (Neb)	SH – 5' – AGT ACA GTC ATC GCG 3' – TCA TGT C**N**G TAG CGC	53.7	0.64 ± 0.14	9.7 ± 2.3

[a]SH - 5' represents $SH(CH_2)_2CONH(CH_2)_6NHCO$ at 5'-OH
[b]Electrochemical detection using 2 μM methylene blue (MB) as redox probe. Q = current at CV peak.
[c]Electrochemical detection with electrocatalysis: 0.5 μM MB, 2 mM $Fe(CN)_6^{3-}$. Q = integrated current at 5s.

appreciably distinguished without electrocatalysis. Figure 2.4 also shows these data in bar graph form, further demonstrating that these lesions, within error, all have the same ability to facilitate CT as a fully matched duplex (TA). When MB is used electrocatalytically, ZA, ZG, and 2Ap are still not distinguishable. Interestingly, FlU or EA incorporation, examined through electrocatalysis, does lead to some attenuation in CT. Table 2.3 summarizes these data and shows melting temperatures for each duplex. All group 3 lesions, with the exception of EA, also show little deviation in melting temperature from a fully matched duplex.

Group 4 Lesions

Group 4 lesions, 5-methyl-cytosine (MC), N6-methyl-adenine (NA), and uracil (UA) are biologically relevant bases that are the product of enzymatic methylation (MC and NA) or polymerase misincorporation (U base paired with A) (*31-33*). Each of these lesions is the result of the addition or subtraction of a methyl group in a location that does not appreciably hinder Watson-Crick hydrogen bonding ability.

Figure 2.5 shows the direct DNA-mediated reduction of MB (without electrocatalysis) measured by cyclic voltammetry. Without electrocatalysis, MB reduction is equivalent for DNAs containing these lesions when compared to a duplex that does not contain any lesions (TA). Figure 2.5 also shows these data as a bar graph, illustrating quantitatively that these lesions are not electrochemically detectable by this method. In addition, data from chronocoulometry experiments using electrocatalysis, our most sensitive assay, show that these lesions are not well detected even when MB is used as a catalytic probe. These data are summarized in Table 2.4. Also shown in Table 2.4 are melting

Figure 2.4. Electrochemical detection of group 3 lesions. A. Cyclic voltammetry without electrocatalysis. B. Bar graph representing peak current attained in cyclic voltammetry experiments without electrocatalysis. C. Chronocoulometry with electrocatalysis. D. Structures of group 3 lesions. Deviations from standard base pairs are shown in red.

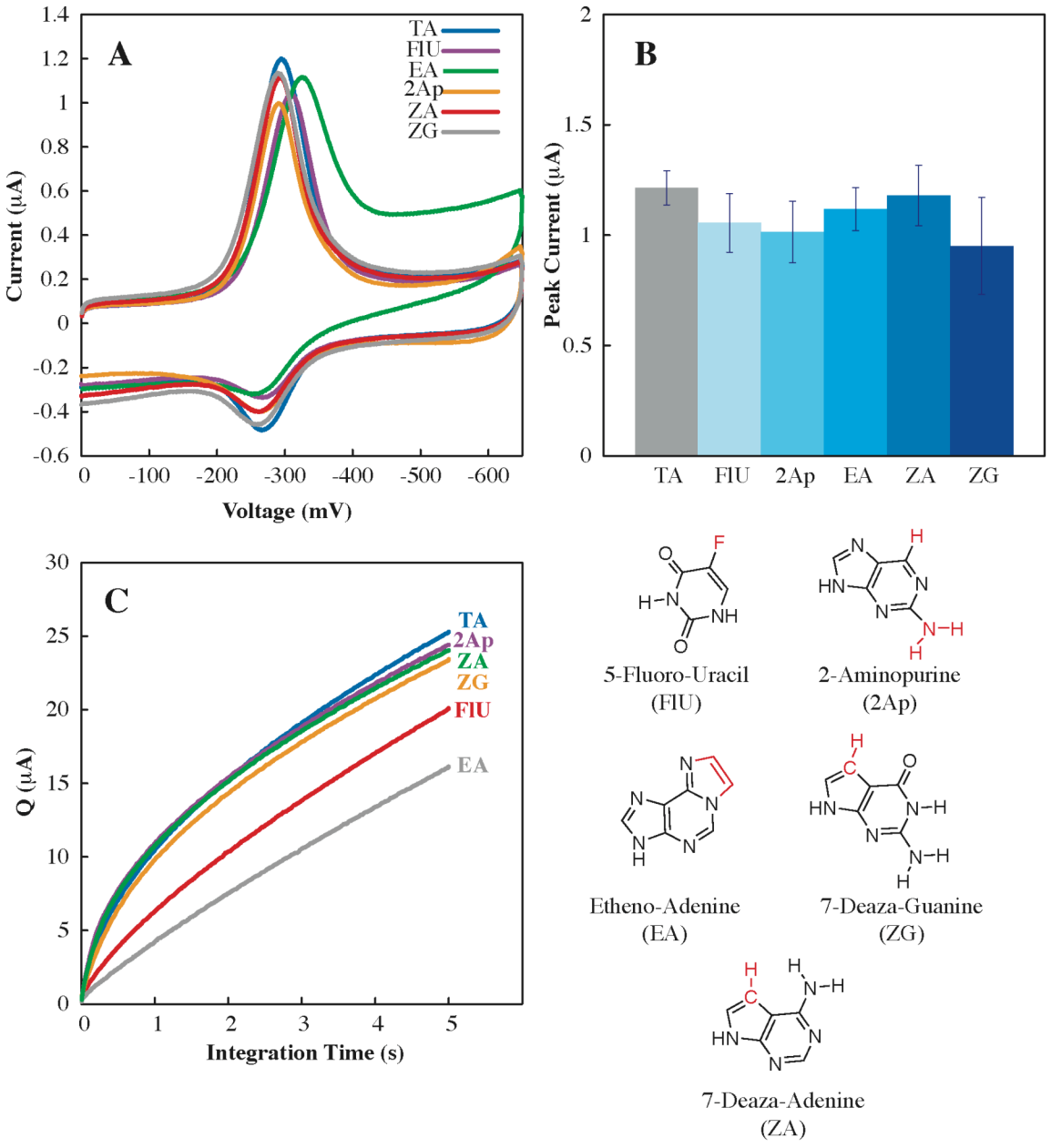

Table 2.3. Electrochemical detection of group 3 lesions.

Lesion	Sequence[a]	T_m (°C)	Q (μA) w/out electrocatalysis[b]	Q (μA) with electrocatalysis[c]
no lesion (TA)	SH – 5' – AGT ACA GTC ATC GCG 3' – TCA TGT CAG TAG CGC	60.0	1.27 ± 0.12	23.9 ± 1.7
5-Fluoro-Uracil (FlU)	SH – 5' – AGT ACA GTC ATC GCG 3' – TCA TGT CAG **U**AG CGC	59.9	1.06 ± 0.13	20.8 ± 0.93
2-Aminopurine (2Ap)	SH – 5' – AGT ACA GTC ATC GCG 3' – TCA TGU C**P**G TAG CGC	57.3	1.01 ± 0.14	20.6 ± 3.3
Etheno-Adenine (EA)	SH – 5' – AGT ACA GTC ATC GCG 3' – TCA TGT C**E**G TAG CGC	50.9	1.12 ± 0.10	18.8 ± 5.1
7-Deaza-Adenine (ZA)	SH – 5' – AGT ACA GTC ATC GCG 3' – TCA TGT C**Z**G TAG CGC	60.0	1.12 ± 0.14	24.5 ± 3.5
7-Deaza-Guanine (ZG)	SH – 5' – AGT ACA GTC ATC GCG 3' – TCA TGT CA**Z** TAG CGC	59.5	0.95 ± 0.22	24.0 ± 1.4

[a]SH - 5' represents $SH(CH_2)_2CONH(CH_2)_6NHCO$ at 5'-OH
[b]Electrochemical detection using 2 μM methylene blue (MB) as redox probe. Q = current at CV peak.
[c]Electrochemical detection with electrocatalysis: 0.5 μM MB, 2 mM $Fe(CN)_6^{3-}$. Q = integrated current at 5s.

Figure 2.5. Electrochemical detection of group 4 lesions. A. Cyclic voltammetry without electrocatalysis. B. Bar graph representing peak current attained in cyclic voltammetry experiments without electrocatalysis. C. Chronocoulometry with electrocatalysis. D. Structures of group 4 lesions. Deviations from standard base pairs are shown in red.

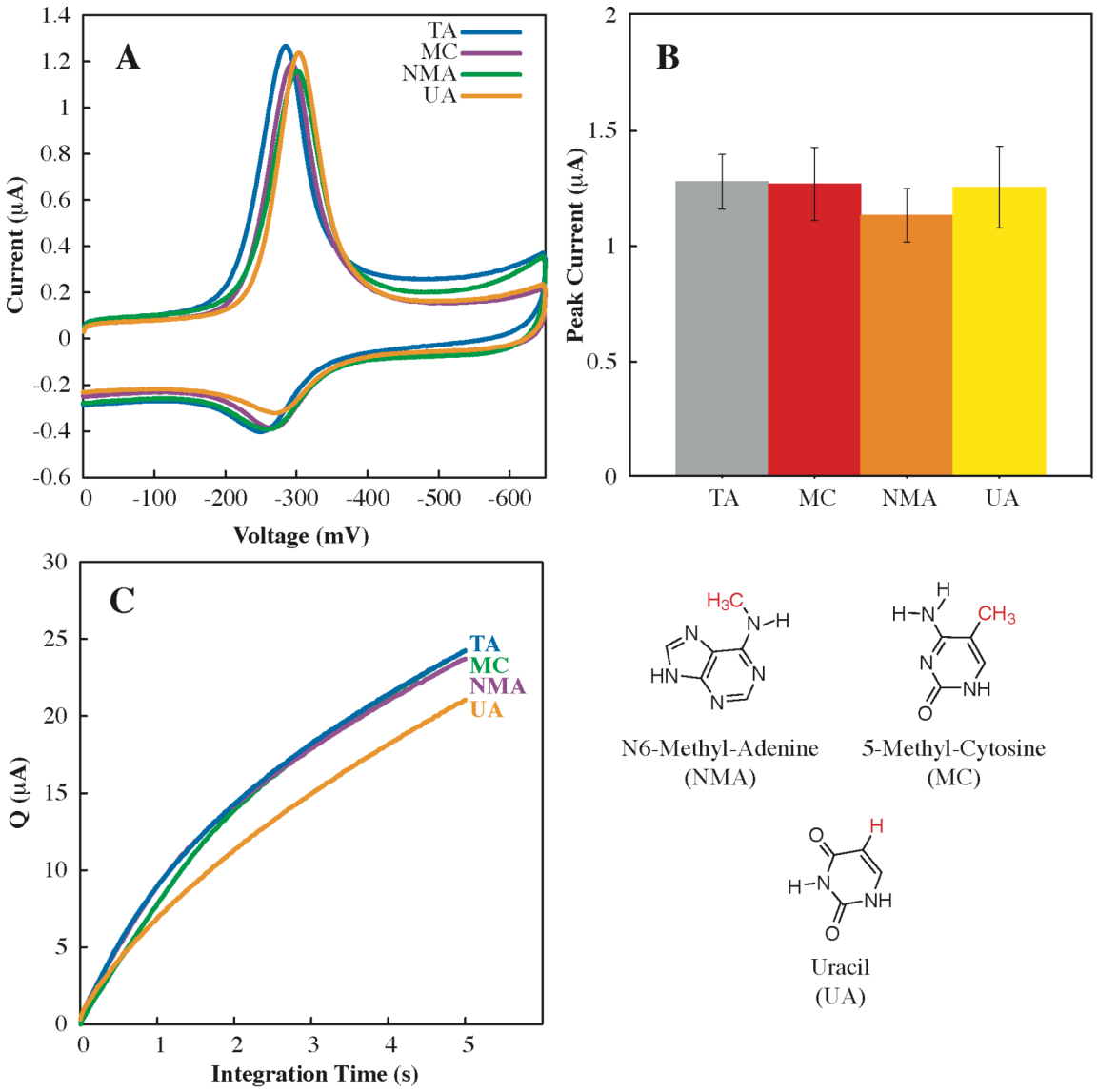

Table 2.4. Electrochemical detection of group 4 lesions.

Lesion	Sequence[a]	T_m (°C)	Q (μA) w/out electrocatalysis[b]	Q (μA) with electrocatalysis[c]
no lesion (TA)	SH – 5' – AGT ACA GTC ATC GCG 3' – TCA TGT CAG TAG CGC	54.3	1.27 ± 0.12	23.9 ± 1.7
5-Methyl-Cytosine (MC)	SH – 5' – AGT ACA GTC ATC GCG 3' – TCA TGT **C**AG TAG CGC	54.3	1.26 ± 0.16	22.8 ± 1.5
Uracil:A (UA)	SH – 5' – AGT ACA GTC ATC GCG 3' – TCA TG**U** CAG TAG CGC	53.2	1.25 ± 0.02	22.4 ± 1.0
N6-Methyl-Adenine (NA)	SH – 5' – AGT ACA GTC ATC GCG 3' – TCA TGT C**A**G TAG CGC	53.1	1.13 ± 0.12	23.47 ± 0.72

[a]SH - 5' represents $SH(CH_2)_2CONH(CH_2)_6NHCO$ at 5'-OH
[b]Electrochemical detection using 2 μM methylene blue (MB) as redox probe. Q = current at CV peak.
[c]Electrochemical detection with electrocatalysis: 0.5 μM MB, 2 mM $Fe(CN)_6^{3-}$. Q = integrated current at 5s.

Figure 2.6. Plot of Q versus ΔT_m based upon data in Tables 1–4. The best linear fit is shown, although $R^2 = 0.57$.

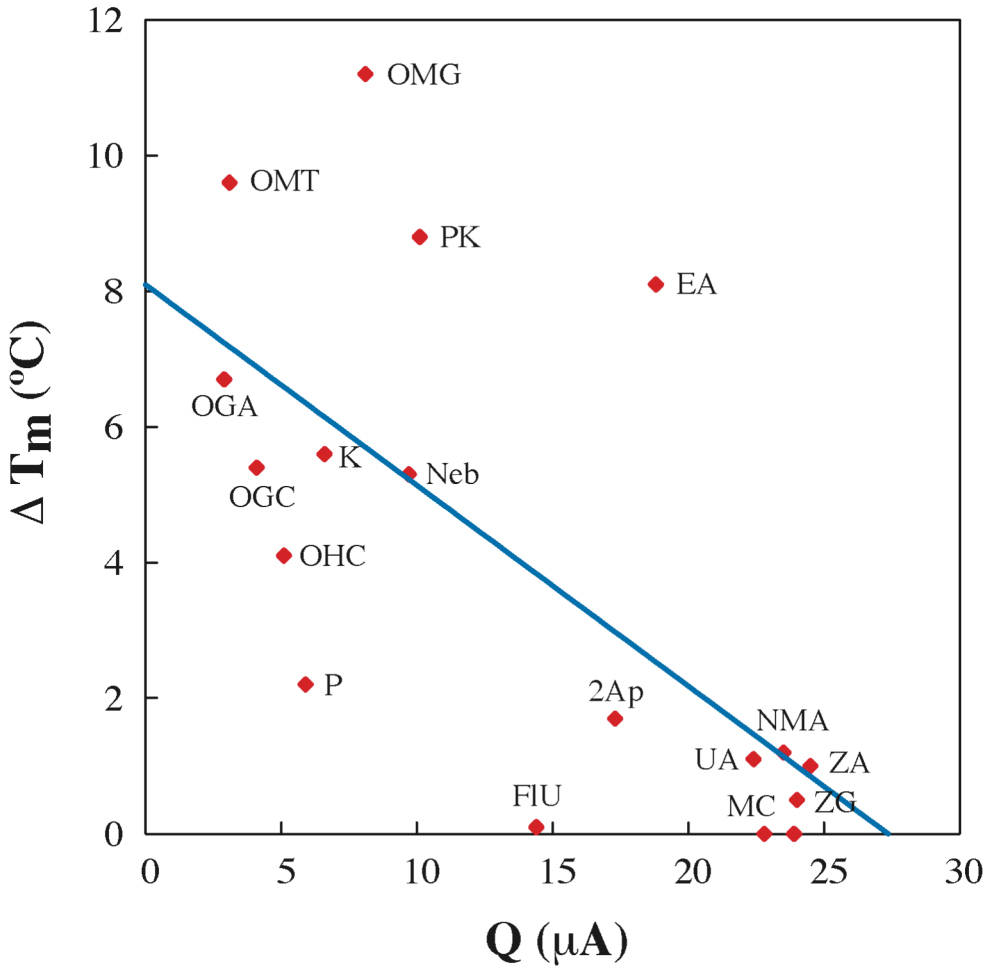

temperatures for these duplexes. It is noteworthy that these lesions do not promote a decrease in melting temperature.

Charge Transfer Efficiency versus Duplex Stability

Figure 2.6 shows a quantitative comparison of melting temperatures for the DNA duplexes, and charge accumulation in the DNA films, our measure of CT efficiency. Integrated charge accumulated after 5s (Q), as measured by our electrochemical assay, is plotted versus the absolute change in T_m from well-matched DNA (TA) for each duplex. The parameter ΔT_m, rather than absolute T_m, is used to account for any differences in experimental conditions among measurements on the lesion-containing DNAs (see Table 2.4). As evident in the plot, little statistical correlation is observed between the CT efficiency and the thermodynamic stability of the duplex; the squared correlation coefficient for these data (R^2) equals 0.57. The electrochemical assay used here depends upon different characteristics of the π-stacked DNA duplex rather than thermodynamic stability.

Discussion

Electrochemical DNA-based biosensors offer a sensitive method for detecting a range of modified bases in DNA. Many of the lesions examined here are implicated in a variety of cancers (*34-36*), so that new assays for low levels of lesions that employ electrocatalysis may provide a novel, early diagnostic tool.

The results presented here also establish the general trends in how base modifications affect CT efficiency. Alteration of the Watson-Crick hydrogen bonding interface yields a profound loss in CT efficiency (OMT, OMG, Neb, P, and K), as does

added steric bulk (P, K, OMT, and OMG). Base structure modifications that may induce base conformation changes (OG:A) also appear to diminish CT in DNA, as do those that place extra hydrophilic groups within the DNA helix (OHC). The presence or absence of methyl groups (MC, NMA, and UA) that do not disrupt hydrogen bonding interactions have little effect on CT efficiency. Little correlation between CT efficiency and thermal stability of duplex DNA containing a particular lesion is evident.

How are these lesions detected within the cell? The lesions examined here fall into three categories: oxidatively damaged bases, alkylated bases, and synthetic base analogues. The bases arising from oxidative or alkylation damage (OHC, OG, OMG, OMT) are all recognized by the cellular repair machinery. Enzymatic recognition by DNA repair systems is considered to involve similar factors to those that affect CT efficiency: hydrogen bonding patterns between the lesion and the opposite base, steric fit, the strength of the glycosidic bond, and base pair dynamics (*37*). OG is thought to be distinguished in part owing to protonation of the N7 nitrogen atom; N7 is not protonated in unmodified guanine (*38*). Repair of OG is also highly dependent on its base pairing environment. For instance, MutY, an enzyme that excises A from OG:A mispairs, can discriminate OG through stacking interactions involving an intercalated tyrosine coupled with hydrogen bonding of the OG to a serine (*39*). OHC is repaired by Endo III, a repair enzyme with a wide substrate specificity that targets oxidized pyrimidines (*40*). With this somewhat non-discriminate enzyme, recognition is thought to involve both the lability of the lesion glycosidic bond and hydrogen bonding of the enzyme with the base opposite the lesion (*41-42*). Direct damage reversal, where aberrant alkylation is transferred from DNA to a reactive cysteine in the repair protein, is the process that repairs O-methylation in DNA (*43*). OMT and OMG are recognized by methyltransferases and these enzymes likely recognize their substrates by sensing the instability of the lesion base pair (*44*). A

consensus has not yet been reached regarding the exact protein/DNA interactions that determine specificity, but structural studies indicate that hydrophobic residues near the reactive cysteine may be involved in recognizing the site of alkylation (*45-46*).

Many of these lesions associated with DNA damage have been previously reported as thermally destabilizing lesions (*47-49*), consistent with our findings here. Base modifications are also associated with dynamic changes in structure. OG is known to switch from the *anti* to the *syn* conformation while pairing with A (*50*). This conformational change is usually invoked as the basis for the mutagenic potential of OG (*51*), but it could also explain the drastic CT efficiency attenuation observed with the OG:A base pair. O-methylation (OMG, OMT) is also known to alter Watson-Crick hydrogen bonding patterns (*48-49*); OMG base paired with C does not form any hydrogen bonds unless C is protonated at the N3 position (*52*). OMT is similarly associated with increased flexibility at the lesion base pair (*49*), a property that, while linked to thermal instability and enzymatic recognition, may also be a factor in attenuation of CT efficiency. Synthetic lesions P, K, and Neb are not targeted by repair systems but can be thermally destabilizing (*24, 53*).

Among the lesions not well-detected in this assay are ZA and ZG, purines where the nitrogen atom at the 7 position is replaced by a carbon atom. This modification is known to lower the redox potential of the base, but the 7-deaza modification is not thought to cause destabilization or altered base pairing and stacking interactions (*54)*. 2-aminopurine base paired with thymine is similarly found to be thermodynamically stable and well stacked in the helix, thus it is not surprising that these three lesions are not easily detected using DNA CT (*5, 55*). FIU, when base paired with adenine, is also thermodynamically stable and not a source of structural distortion (*56*). EA, a sterically bulky lesion, is only marginally detected here. Structural studies indicate that EA forms

no hydrogen bonds with thymine and assumes a nonplanar conformation to accommodate the excess steric bulk of the lesion. Yet the lesion remains intrahelical, does not disrupt the structure of any flanking base pairs, and is purported to have stabilizing stacking interactions both with the bases above and below it and with the thymine opposite (*57*); perhaps these properties are sufficient to allow for some DNA-mediated reduction of MB in the presence of EA. Notably the poor coupling of EA in the base pair stack has been considered to account for the slow rate of base-base CT seen in other studies (*5*).

While O-methylation can be detected through CT, simple base alkylation, MC and NMA, cannot. Enzymatic methylation is generally thought to have a stabilizing effect on duplex DNA (*58-59*). MC can lead to a higher melting temperature for DNA duplexes (*59*) and methylation at the 5 position on the pyrimidine ring, in general, is purported to reduce base pair opening rates (*60*). NMA, also not significantly thermally destabilizing, exhibits more favorable stacking interactions with bases above and below (*58*). Since methylation, if anything, further stabilizes a well-stacked conformation, then, our inability to detect methylation through DNA CT should not be surprising.

Given that DNA CT offers a sensitive strategy to detect a variety of DNA base lesions, might DNA CT chemistry play some role in DNA repair? While recent crystal structures provide some insight into how lesions may be structurally discriminated, in most cases, it is not well understood how DNA damage is first located within the genome; this is especially true in the case of base excision repair, the process that is responsible for removing single instances of base damage (*37*). The results described here certainly support the idea that DNA-mediated CT could potentially provide the foundation for a method of long range detection of DNA damage by repair enzymes. In this context, the detection of 5-hydroxy-cytosine and 8-oxo-guanine is especially

significant as these are substrates for DNA repair glycosylases containing iron-sulfur cofactors that recently have demonstrated redox activity when bound to DNA (*16*).

SUMMARY

Electrochemical DNA-based sensors that exploit the inherent sensitivity of DNA-mediated charge transport (CT) to base pair stacking perturbations are capable of detecting base pair mismatches and some common base damage products. Here, using DNA-modified gold electrodes, monitoring the electrocatalytic reduction of DNA-bound methylene blue, we examine a wide range of base analogues and DNA damage products. Among those detected are base damage products O4-methyl-thymine, O6-methyl-guanine, 8-oxo-guanine, and 5-hydroxy-cytosine, as well as a therapeutic base, nebularine. The efficiency of DNA-mediated CT is found not to depend on the thermodynamic stability of the helix. However, general trends in how base modifications affect CT efficiency are apparent. Modifications of the hydrogen bonding interface in Watson-Crick base pairs yields a substantial loss in CT efficiency, as does added steric bulk. Base structure modifications that may induce base conformational changes also appear to attenuate CT in DNA as do those that bury hydrophilic groups within the DNA helix. Addition and subtraction of methyl groups that do not disrupt hydrogen bonding interactions do not have a large effect on CT efficiency. This sensitive detection methodology based upon DNA-mediated CT may have utility in diagnostic applications and implicates DNA-mediated CT as a possible damage detection mechanism for DNA repair enzymes.

REFERENCES

1. Friedberg, E. C., Walker, G. C., and Siede, W. (1995) *DNA Repair and Mutagenesis* ASM Press.

2. Lindahl, T. (1993) *Nature 362*, 709.

3. Cadet, J., Delatour, T., Douki, T., Gasparutto, D., Pouget, J. P., Ravanat, J. L., and Sauvaigo, S. (1999) *Mutat. Res. 424*, 9.

4. Hemminki, K., Koskinen, M., Rajeniemi, H., and Koskinen, M. (2000) *Regul. Toxicol. Pharmacol. 32*, 264.

5. Kelley, S. O., and Barton, J. K. (1995) *Science 283,* 375.

6. Kelley, S. O., Holmlin, R. E., Stemp, E. D. A., and Barton, J. K. (1997) *J. Am. Chem. Soc. 119*, 9861.

7. Holmlin, R. E., Dandliker, P. J., and Barton, J. K. (1997) *Angew. Chem., Int. Edn. Engl. 36*, 2715.

8. Schuster, G. B. (2000) *Acc. Chem. Res. 33*, 253.

9. Giese, B. (2002) *Annu. Rev. Biochem. 71*, 51.

10. Bhattacharya, P. K., and Barton, J. K. (2001) *J. Am. Chem. Soc. 123*, 8649.

11. Hall, D. B., and Barton, J. K. (1997) *J. Am. Chem. Soc. 119*, 5045.

12. Rajski, S. R., and Barton, J. K. (2001) *Biochemistry 40*, 5556.

13. Boon, E. M., Salas, J. E., and Barton, J. K. (2002) *Nat. Biotech. 20*, 282.

14. Rajski, S. R., Jackson, B. A., and Barton, J. K. (2000) *Mutat. Res. 447*, 49.

15. Friedman, K. A., and Heller, A. (2001) *J. Phys. Chem. B 105*, 11859.

16. Boon, E. M., Livingston, A. L., Chmiel, N. H., David, S. S., and Barton, J. K. (2003) *Proc. Natl. Acad. Sci. U.S.A. 100*, 12543; *ibid. 101,* 4718.

17. Kelley, S. O., Boon, E. M., Barton, J. K., Jackson, N. M., and Hill, M. G. (1999) *Nucleic Acids Res. 27*, 4830.

18. Boon, E. M., Ceres, D. M., Drummond, T. G., Hill, M. G., and Barton, J. K. (2000) *Nat. Biotech. 18*, 1096.

19. Drummond, T.G., Hill, M.G., and Barton, J.K. (2003) *Nature Biotechnology 21*, 1192.

20. Thorp, H. H. (2004) *Topics Curr. Chem. 237,* 159.

21. Boon, E. M., Barton, J. K., Pradeepkumar, P. I., Isaksson, J., Petit, C., and Chattopadhyaya, J. (2003) *Angew. Chem., Int. Ed. Engl. 41*, 3402.

22. Kelley, S. O., Barton, J. K., Jackson, N. M., and Hill, M. G. (1997) *Bioconjugate Chem. 8*, 31.

23. Bjelland, S., and Seeberg, E. (2003) *Mutat. Res. 531*, 37.

24. Hill, F., Loakes, D., and Brown, D. M. (1998) *Proc. Natl. Acad. Sci. U.S.A. 95*, 4258.

25. Brown, G. B., and Weliky, V. S. (1953) *J. Biol. Chem. 204*, 1019.

26. Pratt, W. B., Ruddon, R. W., Ensminger, W. D., and Maybaum, J. (1994) The Anticancer Drugs 2nd ed., Oxford University Press, New York.

27. Ward, D. C., Reich, E., and Stryer, L. (1969) *J. Biol. Chem. 244*, 1228.

28. Barrio, J. R., Secrist, J. A., and Leonard, N. J. (1972) *Biochem. Biophys. Res. Commun. 46*, 597.

29. Latimer, L. J., and Lee, J. S. (1991) *J. Biol. Chem. 266*, 13849.

30. Porello, S. L., Williams, S. D., Kuhn H., Michaels M. L., and David, S. S., (1996) *J. Am. Chem. Soc.118*, 10684.

31. Bird, A. (1992) *Cell 70,* 5.

32. Desrosiers, R., Friderici, K., and Rottman, F. (1974) *Proc. Natl. Acad. Sci. U.S.A. 71*, 3971.

33. Blount, B. C., Mack, M. M., Wehr, C. M., MacGregor, J. T., Hiatt, R. A., Wang, G., Wickramasinghe, S. N., Everson, R. B., and Ames, B. N. (1997) *Proc. Natl. Acad. Sci. U.S.A. 94*, 3290.

34. Goth, R., and Rajewsky, M. F. (1974) *Proc. Natl. Acad. Sci. U.S.A. 71*, 639.

35. Georgiadis, P., Xu, Y. Z., and Swann, P. F. (1991) *Biochemistry 30*, 11725.

36. Olinski, R., Gackowski, D., Rozalski, R., Fokinski, M., and Bialowski, K. (2003) *Mutat. Res. 531*, 177.

37. David, S. S., and Williams, S. D. (1998) *Chem. Rev. 98*, 1221.

38. Bruner, S. D., Norman, D. P. G., and Verdine, G. L. (2000) *Nature 403*, 859.

39. Fromme, C. J., Banarjee, A. A., Huang, S. L., and Verdine, G. L. (2004) *Nature*

427, 652.

40. Hatahett, Z., Kow, Y. W., Purmal, A. A., Cunningham, R. P., Wallace, S. S. (1994) *J. Biol. Chem. 269*, 18814.

41. Fromme, J. C., and Verdine, G. L. (2003) *EMBO J. 22,* 3461.

42. Berdal, K. G., Johansen, R. F., and Seeberg, E. (1998) *EMBO J. 17*, 363.

43. Sassanfar, M., Posanjh, M. K., Essigman, J. M., and Samson, L. (1991) *J. Biol. Chem. 266*, 2767.

44. Duguid, E. M., Mishina, Y., and He, C. (2003) *Chem. Biol. 10*, 827.

45. Daniels, D. S., Mol, C. D., Arvai, A. S., Kanugula, S., Pegg, A. E., and Tainer, J. A. (2000) *EMBO J. 19* 1719.

46. Moore, M. H., Gulbis, J. M., Dodson, E. J., Demple, B., and Moody, P. C. (1994) *EMBO J. 13*, 1495.

47. Oda, Y., Uesugi, S., Ikehara, M., Nishimura, S., Kawase, Y., Ishikawa, H., Inoue, H., and Ohtsuka, E. (1991) *Nucleic Acids Res. 19*, 1407.

48. Gaffney, B. L., and Jones, R. A. (1989) *Biochemistry 28*, 5881.

49. Cruzeiro-Hansson, L., and Goodfellow, J. M. (1994) *Carcinogenesis 15*, 1525.

50. Kouchakdjian, M., Bodepudi, V., Shibutani, S., Eisenberg, M., Johnson, F., Grollman, A. P., and Patel, D. J. (1991) *Biochemistry 30*, 1403.

51. Cheng, K. C., Cahill, D. S., Kasai, H., Nishimura, S., and Loeb, L. A. (1992) *J. Biol. Chem. 267*, 166.

52. Williams, L. D., and Shaw, B. R. (1987) *Proc. Natl. Acad. Sci. U.S.A. 84,* 1779.

53. Jiricny, J., Wood, S. G., Martin, D., and Ubasawa, A. (1986) *Nucleic Acids Res. 14*, 6579.

54. Baik, M., Silverman, J. S., Yang, I. V., Ropp, P. A., Szalai, V. A., Yang, W., and Thorp, H. H. (2001) *J. Phys. Chem. B 105,* 6437.

55. Law, S.M., Eritja, R., Goodman, M.F., and Breslauer, K.J. (1996) *Biochemistry 35*, 12329.

56. Kramer, A. B., Mikita, T., and Beardsley, G. P. (1987) *Biochemistry 26*, 391.

57. Kouchakdjian, M., Eisenberg, M., Yarema, K., Basu, A., Essigmann, J., and Patel, D. J. (1991) *Biochemistry 30*, 1820.

58. Engel, J. D., and von Hippel, P. H. (1977) *J. Biol. Chem. 253*, 927.

59. Marcourt, L., Cordier, C., Couesnon, T., and Dodin, G. (1999) *Eur. J. Biochem. 265*, 1032.

60. Warmlander, S., Sponer, J. E., Sponer, J., and Leijon, M. (2002) *J. Biol. Chem. 277*, 28491.